〈系统与设计〉

Research of Attitude Measuring System Using Single Camera for Non-cooperative Spacecraft

LI You-wen，ZHANG Xi-tao，ZHANG Xue-feng
(*Luoyang Opto-Electro Technology Development Center, Luoyang* 471009, *China*)

Abstract：In this paper, the attitude measuring system using single camera for the non-cooperative spacecraft is researched. The basic principle of attitude measuring theory is deeply studied, and also the advantages and disadvantages of traditional attitude measuring method, which is based on cooperative target and double camera, are listed for comparison. The mathematical model of the perspective camera is established with the matching points. The attitude is measured by the method of Epipolar Geometry. It is proved that, the theory of attitude measuring system is available according to the experimental results. It puts forward a new research approach for the guidance system to indentify the target attitude automatically.
Key words：matching，non-cooperative，attitude measurement

基于单目相机的空间非合作目标姿态测量

李又文，张喜涛，张学锋
（中国空空导弹研究院，河南 洛阳 471009）

摘要：提出了一种基于单目相机的空间非合作目标姿态测量方法。研究了目标姿态测量的基本原理并介绍了基于合作目标和双目相机的优缺点。通过匹配点得到相机的参数模型，然后利用对极几何方法得到目标姿态。仿真实验表明本文方法能够估计目标的姿态，为导引系统提供了一种自动获取目标姿态信息的新方法。
关键词：匹配；非合作；姿态测量
中图分类号：V476 **文献标识码**：A **文章编号**：1001-8891(2014)02-0110-05

0 Introduction

Among all kinds of key technologies to precisely capture a target in outer space, the guidance mode based on material analysis and attitude measuring system is gradually becoming the research focus in the development of precisely guided weapon. This system mainly deals with typical targets with long distance, such as satellite, cloud stone and so on. In order to achieve precise capture to targets in outer space, it is an absolutely necessary step to identify the attitude information of the target.

Based on the relationship between the measuring system and the target, the process and the primary methods are divided into two classes, used in cooperative and non-cooperative target[1-2]. The former class is realized by artificial points, the target's image library, 3d model, communication with the target and so on. This method is simple, maturity and reliable. But it's limited by the application range. The last method does without the information from the target. It mainly includes four kinds of measuring system, such as Satellite Navigation System, microwave radar system, lidar system and optical imager system. And the optical imager system has the attention of researchers because of its advantages of cost, skill and volume.

With the development of the computer vision, non-cooperative measuring system is promoted. For example, Canadian NFAS vision system replaces the

收稿日期：2013-10-09；修订日期：2013-12-26.
作者简介：李又文（1979-）男，职称：工程师，主要研究方向：图像处理；E-mail：cama014@163.com。

method of 3d model with two cameras' reconstruction[3]. Although realizing non-cooperative measure, the system has an obviously limitation, such as short work distance, short base line, large work flat and so on. To overcome this problem, this paper introduces a new measuring method by dealing with the Image sequence gained from a single camera.

1 Matching Algorithm

The most commonly used matching algorithm is SIFT. For it is difficult to directly acquire the information of the SIFT with small target, we need to deal it with the method of pixel contrasting. And it can shorten the time of SIFT with the method of up sampling when the target is large.

The SIFT algorithm operates in four steps to detect and describe local features, or key points, in an image:

1) Scale-space extrema detection[4]

The SIFT algorithm begins by identifying the locations of candidate key points as the local maxima and minima of a difference-of-Gaussian pyramid that approximates the second-order derivatives of the image's scale space.

2) Key point localization and filtering[5]

After candidate key points are identified, their locations in scale space are interpolated to sub-unit accuracy. The interpolated key points, which is potential instability, are rejected with low contrast or a high edge response-computed based on the ratio of principal curvatures.

3) Orientation assignment[6]

The key points that survive filtering are assigned one or more canonical orientations based on the dominant directions of the local scale-space gradients. After orientation assignment, each key point's descriptor can be computed relative to the key point's location, scale and orientation to provide invariance to these transformations.

4) Descriptor computation[7]

Finally, a descriptor is computed for each key point by partitioning the scale-space region around the key point into a grid, computing a histogram of local gradient directions within each grid square, and concatenating those histograms into a vector. To provide invariance to illumination change, each descriptor vector is normalized to unit length, and reduced the influence of large gradient values, and then renormalized.

2 Wrong Match Pairs Elimination

The epipolar geometry is the intrinsic projective geometry between two views. It is independent of scene structure, and only depends on the cameras' internal parameters and relative pose. It is in nature the geometry of the intersection of the image planes with the pencil of planes having the baseline as axis(the baseline is the line joining the camera centres). This geometry is usually motivated by considering the search for corresponding points in matching.

2.1 Fundamental Matrix

The fundamental matrix $\boldsymbol{F}$ encapsulates this intrinsic geometry. It is the algebraic representation of epipolar geometry. Suppose a point X in 3-space, which is shown in Figure 1, is imaged in two views, at x in the first, and x' in the second. The two cameras are indicated by their centers C and C'. The camera centers, 3-space point X, and its images x and x' lie in a common plane. The image point x back-projects to a ray in 3-space defined by the first camera centre, C and x. This ray is imaged as a line l' in the second view. The 3-space point X which projects to x must lie on this ray[8].

$$l' = \boldsymbol{F}x \tag{1}$$

The line l'in the second view is obtained by joining x' to the epipole e'.

$$x'^{T}l' = 0 \tag{2}$$

And according to formula (1) and (2) we can get:

$$x'^{T}\boldsymbol{F}x = 0 \tag{3}$$

We can compute the fundamental matrix $\boldsymbol{F}$ by the method of RANSAC, 8-point algorithm, algebraic minimization algorithm and so on[9].

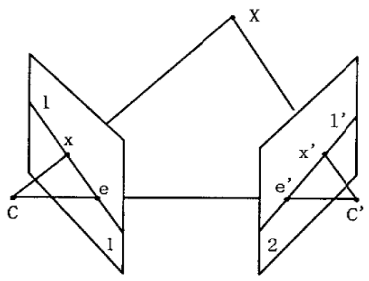

Fig.1 Epipolar geometry

2.2 RANSAC

The following steps is repeated for N samples, which is determined adaptively by the number of points[10].

1) Select a random sample of 8 correspondences and compute the fundamental matrix $\boldsymbol{F}$ by the method of 8 point algorithm.

2) Calculate the distance d for each putative correspondence.

3) Compute the number of inliers consistent with $\boldsymbol{F}$ by the number of correspondences for which $d<d_T$ pixels.

The $\boldsymbol{F}$ is chosen with the largest number of inliers. And the inliers are the correct matching points[11].

3 Attitude Measurement

The most commonly used imaging model concerning machine vision technology is fluoroscopy camera model. It meets the following projection equation:

$$x=\boldsymbol{P}X \tag{4}$$

During the above formula, $\boldsymbol{P}$ is a 3×4 homogeneous matrix. In Euclidean reconstruction, $\boldsymbol{P}$ can be expressed as:

$$\boldsymbol{P}=KR^T[I|-t] \tag{5}$$

During the above formula, $\boldsymbol{K}=\begin{bmatrix} f & s & u \\ 0 & af & v \\ 0 & 0 & 1 \end{bmatrix}$, $\boldsymbol{R}=\begin{bmatrix} r_{11} & r_{12} & r_{13} \\ r_{21} & r_{22} & r_{23} \\ r_{31} & r_{32} & r_{33} \end{bmatrix}$, $t=\begin{bmatrix} t_1 \\ t_2 \\ t_3 \end{bmatrix}$. K is the inner orientation elements of a camera, f is the focal length, a is the aspect ratio, s is the distortion factor, $[u\ v]$ is the image principal point. Usually, $s=0$, $a=1$, and the image principal point is also close to the image geometric center. $\boldsymbol{R}$ and $\boldsymbol{t}$ are respectively the rotation matrix and translation matrix relatively to the 3-space coordinate.

Assume the matrix $\boldsymbol{P}^+=\boldsymbol{P}^T(\boldsymbol{P}\boldsymbol{P}^T)^{-1}$, and based on the formula (4), The image point x'' projected by the point $\boldsymbol{P}^+x$ is on the line l' in the second image. We can get:

$$l'=e'\cdot x''=(\boldsymbol{P}'\boldsymbol{C})(\boldsymbol{P}'\boldsymbol{P}^+x) \tag{6}$$

Assume that the 3-space coordinate's center point is in coincidence to the camera principal point in the first image. The two homogeneous matrixes can be expressed as:

$$\boldsymbol{P}=KR^T[I|\ 0] \tag{7}$$

$$\boldsymbol{P}'=K'R^T[I|-t] \tag{8}$$

$$\boldsymbol{C}=\begin{bmatrix} 0 \\ 1 \end{bmatrix} \tag{9}$$

$$\boldsymbol{P}'=\begin{bmatrix} K^{-1} \\ 0 \end{bmatrix} \tag{10}$$

Substitute formula (7), (8), (9), (10) into formula (6), we can get:

$$\boldsymbol{F}=\boldsymbol{P}'\boldsymbol{C}(\boldsymbol{P}'\boldsymbol{P}^+)=[\boldsymbol{P}'\boldsymbol{C}]_X\,\boldsymbol{P}'\boldsymbol{P}^+=K'^{-T}[\boldsymbol{t}]_XRK^{-1} \tag{11}$$

Assume the essential matrix $\boldsymbol{E}=[\boldsymbol{t}]_XR$, we can get:

$$\boldsymbol{E}=K'^T\boldsymbol{F}K \tag{12}$$

Suppose that matrix $\boldsymbol{W}=\begin{bmatrix} 0 & -1 & 0 \\ 1 & 0 & 0 \\ 0 & 0 & 1 \end{bmatrix}$ and the SVD of $\boldsymbol{E}$ is $\boldsymbol{U}$ diag(1,1,0)V^T, we gain two possible factorizations as follows:

$$t=\pm U(0,\ 0,\ 1)^T=u_3 \tag{13}$$

$$\boldsymbol{R}=\boldsymbol{U}\boldsymbol{W}V^T \tag{14}$$

$$\boldsymbol{R}=\boldsymbol{U}\boldsymbol{W}^TV^T \tag{15}$$

Substitute formula(11)、(13)、(14)、(15) and a pair of matching points into formula(3), we can choose the correct matrix $\boldsymbol{R}$.

4 Experiment and Results

4.1 Image Generation and Camera Calibration

In simulation testing, we get image sequences by camera model and satellite model created by 3ds max which is shown in Figure 2.

Combined with Zhang's classic calibration algorithm[12], we get the inner matrix (see Table 1) based on the LM optimized method[13] and the calibration plate which is shown in Figure 3.

$$\boldsymbol{K}=\begin{bmatrix} 378290.3 & 0 & 1392.5 \\ 0 & 375741.3 & 1042 \\ 0 & 0 & 1 \end{bmatrix}$$

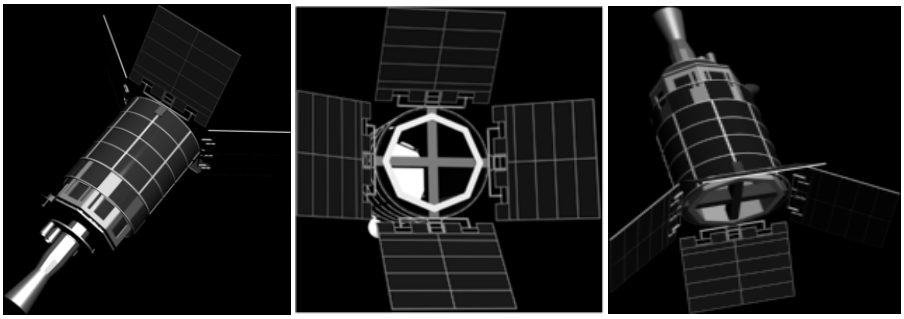

Fig.2 Satellite model

Table 1 Camera and satellite model parameters

Camera model	Satellite model
Focus: 5 m	Length: 6.5 m
Resolute: 2786×2085	Width: 6.5 m
	Height: 8.0 m

Fig.3 Calibration plate

4.2 Point Extraction and Matching

We use the SIFT and RANSAC method to match the satellite in two images, which is shown in Figure.4 (up). And the enlarge image is in Figure 4 (left-down). By using of the method of 8 point algorithm, which is drawn in Figure 3(right-down), we can get the fundamental matrix.

4.3 Attitude Measurement

Revolving the satellite by pitching angle, and moving the satellite to approach the camera from 5 km to 150 km, we can get the test results which are shown in Table 2.

Revolving the satellite by rolling angle, and moving the satellite to approach the camera from 5km to 150km, we can get the test results which are shown in Table 3.

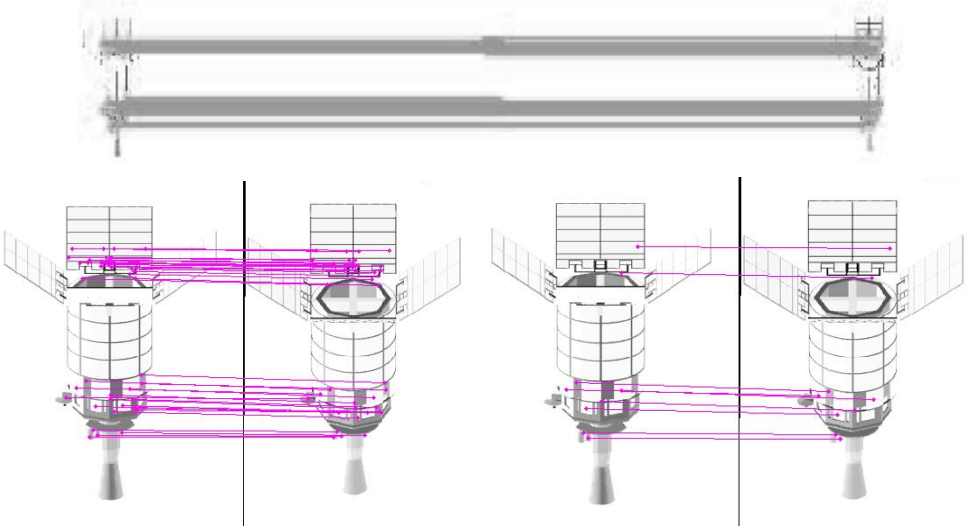

Fig.4 Matching results

Table 2 Pitching angle errors of the test results

Angle	Distance	Pixels	Match Pairs	Results	Error
174 mrad	150 km	125	15	249 mrad	75 mrad
174 mrad	50 km	1238	9	27 mrad	147 mrad
174 mrad	40 km	2125	10	75 mrad	99 mrad
174 mrad	30 km	7330	15	78 mrad	96 mrad
174 mrad	20 km	11672	14	207 mrad	33 mrad
174 mrad	10 km	31894	44	127 mrad	47 mrad
174 mrad	5 km	201892	57	167 mrad	7 mrad

Table 3 Rolling angle errors of the test results

Angle	Distance	Pixels	Match Pairs	Results	Error
174 mrad	150 km	153	14	243 mrad	69 mrad
174 mrad	50 km	2081	8	290 mrad	116 mrad
174 mrad	40 km	3950	11	202 mrad	28 mrad
174 mrad	30 km	5760	32	200 mrad	26 mrad
174 mrad	20 km	10447	34	188 mrad	14 mrad
174 mrad	10 km	39286	87	198 mrad	24 mrad
174 mrad	5 km	148320	210	134 mrad	40 mrad

Experimental results with less than 200 pixels and 150 km clearly demonstrate the validity of small target detection. And the match pairs show that the method is efficient to feature point extraction. From table 2 and table 3, we can see, the contrastive simulation on the error is carried to show the accuracy of the attitude estimation. Due to the method of pixel contrasting, the errors of the angle in the distance of 150 km are less comparing to errors with short distance. The angle errors come down with the distance turning short in the whole.

References:

[1] 张世杰, 谭校纳, 曹喜滨. 非合作航天器相对位姿的鲁棒视觉确定方法[J]. **哈尔滨工业大学学报**, 2009, **41**(7):6-10.

[2] 周军, 白博, 于晓洲. 一种非合作目标相对位置和姿态确定方法[J]. **宇航学报**, 2011, **32**(3):516-512.

[3] Anderson M, Nordhind P, Ekhindh J O. Modeling, matching and tracking for the strieovision II project: State-of-the-Art-Review[R]. Technical Report TRITA-NA-P9321, Dept. of Numerical Aralysis and Computing Scierce, Royal Institute of Technology, June 1993.

[4] Brown M, Lowe D G. Invariant features from interest point groups[C]//*British Machine Vision Conference*, Cardiff, Wales, 2002: 656-665.

[5] Lowe D G. Distinctive image features from scale-invariant keypoints[J]. *International Journal of Computer Vision*, 2004, **60**(2): 91-110.

[6] Lowe D G. Object recongnition from local scale invariant features[C]//*Proceedings of the Seventh International Conference on Computer Vision*(ICCV'99), Kerkyra, Greece, 1999: 1150-1157.

[7] Mikolajczyk K, Schmid C. A Performance Evaluation of Local D escriptors[C]//*Proceedings of the Conference on Computer Vision and Pattern Recognition*. Madison, Wisconsin, USA: [s. n.], 2005: 257-264.

[8] Hartley R, Zisserman A. *Multiple view geometry in computer Vision*[M]. Second, New York: Cambridge University Press, 2003: 239-250.

[9] R Hartley. In defence of the 8-point algorithm[C]//*Proceedings of the Fifth International Conference on Computer Vision*, 1995: 1064-1070.

[10] Fischler M A, Bolles R C. Random sample consensus: a paradigm for model fitting with applications to image analysis and automated cartography[J]. *Communication of ACM*, 1981, **24**(6): 381-395.

[11] Torr P, Murray D. The development and comparison of robust methods for estimating the fundamental matrix[J]. *Int. Journal of Computer Vision*, 1997, **24**(3): 271-300.

[12] Zhang Zhengyou. A Flexible New Technique for Camera Calibration[J]. *IEEE. Transactions on Pattern Analysis and Machine Intelligence*, 2000, **22**(11): 1330-1334.

[13] Sainz M, Bagherzadeh N, Susin A .Recovering 3D metric structure and motion from multiple uncalibrated cameras[C]//*Proc. of the International Conference on Information Technology*: *Coding and Computing*. [S.l.]: IEEE Press, 2002: 268-273.